Sulfur-Doped Silicon Photodiode by Ion Implantation and Femtosecond Laser Annealing

Chun-Hao Li, Ji-Hong Zhao, *Member, IEEE*, Xin-Yue Yu, Qi-Dai Chen, Jing Feng, Pei-De Han, and Hong-Bo Sun, *Member, IEEE*

Abstract—Femtosecond (fs) laser annealing has been applied to improve the crystalline quality and absorptance below bandgap of ion implanted silicon (Si) with sulfur (S). The doping concentration of S is up to 10^{20} atoms/cm^3, which is at least four orders of magnitude higher than the solid solubility of S in crystalline Si. According to the Raman spectra, after fs laser irradiation with appropriate laser energy, the crystal quality is evidently better than primary ion implanted sample. Moreover, the optical absorption coefficient at wavelengths of 1100~2400 nm is up to 1.54×10^4 cm^{-1}, which is much larger than the contribution of free carriers. Excessive laser energy will induce serious ablation effect and cause the removing of doping layer. We consider that the high absorption is a combination of sub-bandgap transition of S-related localized states, free carrier absorption, ion implantation induced defect absorption and fs laser irradiation induced defect absorption. In the end, a photoresponse of 8.4 mA/W is obtained for the photodiode for 1310 nm detection light.

Index Terms—Femtosecond laser, ion implantation, infrared absorption, sulfur doping, photo-detection.

I. INTRODUCTION

IN RECENT years, an increasing number of researchers have put their interests on fabricating a kind of silicon (Si) materials with high sub-bandgap absorption [1]–[9]. There are two typical methods to form this material. In the first method, textured and supersaturated Si is realized by one step pulsed laser microstructuring [1]–[5]. In the second method, the sub-bandgap absorption of Si is improved by the combination of ion implantation and nanosecond (ns) laser melting process [6]–[9]. However, the Si materials with high infrared absorption prepared by both methods still have some weaknesses. For femtosecond (fs) laser irradiated Si (black Si), the surface microstructures and crystallographic disordered layer are produced during the supersaturation doping process. Although the photodiode fabricated by fs irradiated black Si can obtain a high gain and has a very sensitive response to photo energy above bandgap, the research on photodiode that can detect the photo energy below bandgap is still underway [10], [11].

In addition, the observed infrared absorption of sulfur (S)-doped microstructured Si has not been explained very well. Compared with the fs laser irradiated samples, Si materials prepared by the combination of ion implantation and ns laser melting exhibits higher crystalline quality and lower surface roughness. But this material possesses a very low absorption below bandgap after thermal annealing, which restricts this material's application in infrared detection [6]. Here we will report a new method to fabricate S-doped supersaturated Si material with high absorption below bandgap by ion implantation and fs laser annealing technique. Moreover, the infrared photodiode devices based on these materials are produced.

II. EXPERIMENTS

After a standard cleaning solution treatment [12], Si (100) wafers (n-type, $\rho = 5\sim10$ $\Omega\cdot$cm, 280 μm thick, single-side polished) are ion implanted with 30 keV 32S$^+$ to a dose of 1.0×10^{15} ions/cm^2 at an incident angle of 7°. Then the ion implanted samples are irradiated by Ti:Sapphire femtosecond laser amplifier (Spectra-Physics) with 800 nm center wavelength, 100 fs pulse duration, and 2.5 kHz repetition rate. Laser spot is focused to 260 μm through a lens with 600 mm focal distance. Laser fluences of 1 kJ/m^2 and 3 kJ/m^2 are selected. In order to get sufficiently large surface area (15×15 mm^2) for spectroscopic measurements of optical reflection and transmission, the ion implanted samples are installed into a vacuum chamber; then this chamber is fixed on a three-dimensional translation stage which can be controlled by computer program. Before laser irradiation, the vacuum chamber is evacuated to 5 Pa and filled by argon atmosphere of 0.1 MPa. Finally, the whole area of ion implanted Si is irradiated by translating the vacuum chamber, together with the Si wafer, in S-line sweep during pulsed laser irradiation. The line scanning speed is set to 0.5 mm/s or 2.0 mm/s, and the corresponding average number of pulse shots on each point is 500 or 1000, respectively. The Raman spectra are obtained by LabRAM HR Evolution Raman Spectrometer (HORIBA Scientific) with a 532 nm laser. The surface morphologies of the ion implanted Si and fs laser irradiated Si have been detected by Atomic Force Microscope (AFM, Bruker Dimension Icon, Germany) in tapping mode and a field-emission scanning electron microscope (SEM, JSM-7500F, JEOL, Japan). The IR absorption spectra (1100~2400 nm) of ion implanted and fs laser annealed Si samples are measured indirectly using a spectrophotometer (Shimadzu UV-3600 equipped with an integrating sphere LISR-UV3100). Actually the total absorptance A (A=1−T−R) is calculated from the measured transmittance T and reflectance
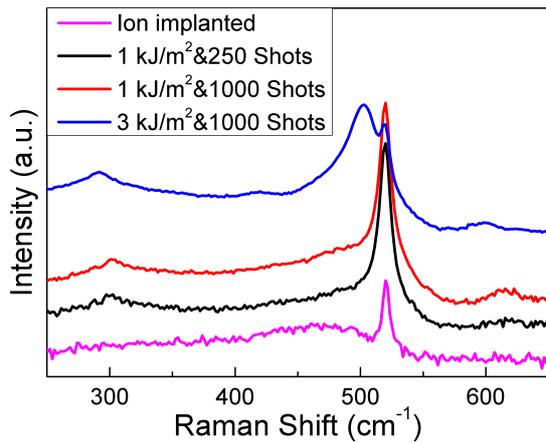
Fig. 1. Raman spectrum of ion implanted Si samples with dose of 1.0×10^{15} ions/cm^2 after fs laser process.

R (including hemispherical specular and diffuse) which can be directly obtained by the instruments. The S content is determined by secondary ion mass spectroscopy (SIMS) equipped with a CAMECA 4f device using 14.5 keV Cs$^+$ primary beam at an incident angle of 30° from the surface normal and monitoring the 32S secondary ions.

III. RESULTS AND DISCUSSION

The Raman spectra of ion implanted Si samples after fs laser treatment are shown in Fig. 1. Here, the Si-I peaks (300 cm^{-1} and 520 cm^{-1}) exist for all samples (ion implanted samples after fs laser treatment) in the Raman spectra. As shown in Fig.1, the ion implanted sample (the pink line) presents a new phase of amorphous Si (α-Si broad vibration peak at 475 cm^{-1}) due to the strong surface damage induced by ion bombing [13], [14]. After irradiating with proper fs laser fluence (1 kJ/m^2, the dark and red lines), the α-Si vibration peak of ion implanted Si disappears. However, when laser irradiation energy increase to 3 kJ/m^2(the blue line), not only the damaged lattice cannot be repaired, but also there are new phases in fs laser treated samples. These unwanted new phases include a strong variation peak at 502 cm^{-1} which is likely to be Si nanocrystal and a weak variation peak at 419 cm^{-1} that may come from polycrystalline Si [15]. From Fig. 1, we can figure out that proper fs laser fluence can transform the α-Si into crystalline Si. In order to avoid inducing other unwanted phases during fs laser treatment, the ion implanted samples irradiated with fs laser fluence of 1 kJ/m^2 are further investigated.

The surface morphology of ion implanted Si and the samples after fs laser annealing are compared with undisturbed Si substrate. The AFM micrographics are showed in Fig. 2. The Si substrate (Fig. 2a) and ion implanted Si (Fig. 2b) present a perfect smoothness and homogeneous roughness. The RMS roughness of Si substrate and ion implanted Si are 0.363 nm and 0.677 nm, respectively. However, the melting and ablating effect of fs laser with a fluence of 1 kJ/m^2 can obviously increase the roughness of ion implanted Si, which shows as the SEM images in Fig. 2c and Fig. 2d. From the SEM images of fs laser treated samples, we can find that
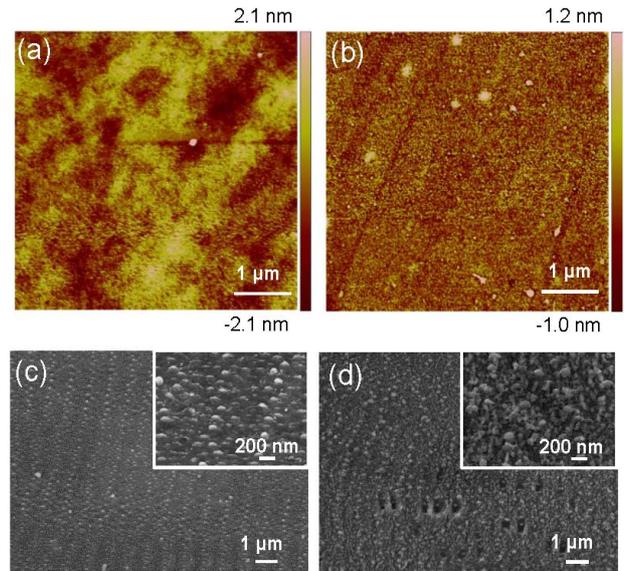

Fig. 2. AFM micrographics of (a) $\sim$ (b) and SEM images of (c) and (d). AFM micrograph of Si substrate (a); AFM micrograph of ion implanted Si (b); SEM images of fs laser treated Si with flunce of 1kJ/m^2 and 250 shots (c); SEM images of fs laser treated Si with flunce of 1kJ/m^2 and 1000 shots (d).
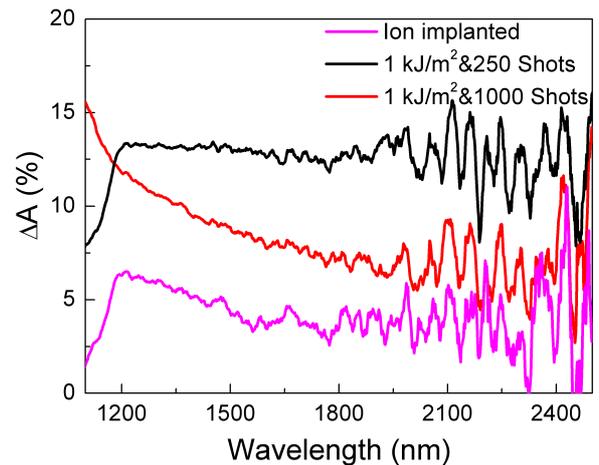

Fig. 3. Relative absorptance ΔA in IR wavelengths (1100$\sim$2400 nm) of ion implanted and fs laser annealed Si.

ripple nanostructures with periodical arrangement are formed on Si surface and the height of the structures is between 100 and 300 nm. The partial enlarged details of inset pictures in Fig. 2c and Fig. 2d show that the surface with nanostructures is not uniform and the periodicity is not strict, too. Combining with the Raman spectra in Fig. 1, we can draw the conclusion that the increasing of surface roughness and formation of nanostructures after fs laser treating does not seriously affects the crystalline quality of ion implanted Si. In addition, the formation of nanostructures may improve the absorption of Si below bandgap due to the light trapping effect of structured surface.

The relative absorptance ΔA of S-doped Si layer was defined to $\Delta A = A_S - A_B$, where A_S and A_B represent the absorptance of S-doped Si samples (before and after fs laser annealing) and bare Si substrate, respectively. The ΔA of S-doped Si samples is shown in Fig. 3. There is a small
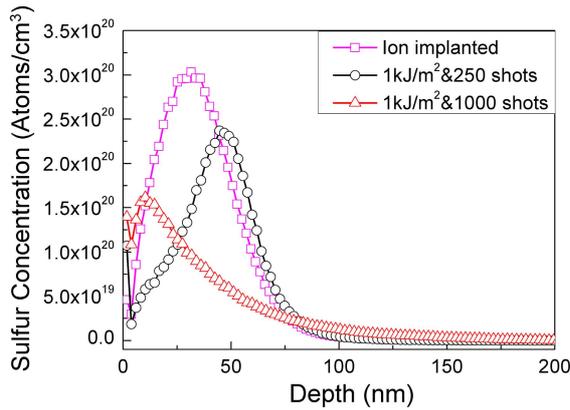
Fig. 4. SIMS depth profiles for ion implanted and fs laser irradiated Si samples.

Fig. 5. The absorption coefficient of S-doped layer, which has deducted the absorption from bare Si substrate.

enhancement in the absorptance of ion implanted Si sample at wavelengths of 1100 nm $\sim$ 2400 nm. Such a low absorption enhancement is due to the fact that the lowest-energy state of amorphous Si:S has twofold coordinated S and is transparent at these wavebands [16]. However, the absorptance of ion implanted Si is increased by fs laser irradiation and the crystalline quality is improved by laser melting and rapid solidification process (1 kJ/m^2&250 shots). As is well known, S in crystalline Si prefers to occupy substitutional sites, which will create deep levels and lead to optical absorption [16]. However, more deposit pulses do not continually improve the absorptance below bandgap of ion implanted Si because of a strong negative effect of ablation (1kJ/m^2&1000 shots). We should note that, once the laser ablation process is induced, the supersaturated Si layer, which contributes to the below bandgap absorption will be removed simultaneously.

The S concentration-depth profiles are shown in Fig. 4. According to the simulation result, the maximum implantation depth in Si for S implanted at 30 keV is 41 nm [17]. The maximum S atom concentration for the implanted dose of 1.0×10^{15} ions/cm^2 is approximately 2.27×10^{20} cm^{-3}, which is at least four orders of magnitude above the equilibrium solubility limit of S in Si [18]. From the SIMS result in Fig. 4, the measured maximum implantation depth and maximum S atom concentration of ion implanted Si are 29.8 nm and 2.95×10^{20} cm^{-3}, which are very close to the theoretical simulation parts. There is an abrupt drop in S concentration at 47.3 nm for the sample irradiated with 1kJ/m^2 and 250 shots. We considered that the drift of doping depth is corresponding to the maximum penetration of the melt front during fs laser irradiation [19]. Then the coming rapid solidification will lead to a trapping of high supersaturated substitutional dopants in Si crystal. In contrast, for 1kJ/m^2 and 1000 shots irradiated sample, the peak concentration of S atoms and maximum implant depth are reduced to 1.6×10^{20} cm^{-3} and 10.3 nm, respectively. This is caused by the partially removal of the surface layer of the S implant layer by laser ablation effect.

The pure absorption coefficient induced in supersaturated doping layer (don't include Si substrate) is defined as $\Delta\alpha = (\alpha - \alpha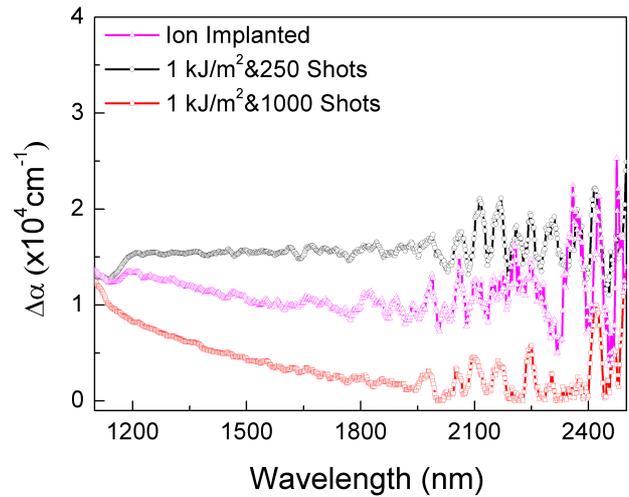_{sub})d/d'$. α represents the absorption coefficient of ion implanted samples after fs laser annealing and is calculated by $\alpha = (1/d)\ln[(1-R)/T]$, α_{sub} is the absorption coefficient of Si substrate; d is thickness of Si substrate, d' is the depth of supersaturated doping layer and it is about 300 nm obtained from SIMS profiles since the concentration of S dropped to 10^{15} cm^{-3} at depth of 300 nm for all samples. Finally, the calculated pure absorption coefficient $\Delta\alpha$ at wavelengths of 1100$\sim$2400 nm contributed by supersaturated doping layer is shown as Fig. 5.

The $\Delta\alpha$ at 1310 nm of 1kJ/m^2 & 250 shots irradiated sample and ion implanted sample are 1.54×10^4 cm^{-1} and 1.27×10^4 cm^{-1}, respectively. According to Spitzer's and Fan's reports, the maximum anticipated value of absorption coefficient of Si is about 200 cm^{-1} for a carrier concentration of 10^{19} cm^{-3}@1310 nm [6], [21]. And the free carrier absorption coefficient at this wavelength is linearly proportional to the free electron concentration for shallow donor impurities (such as As and P) [21]. In addition, after Hall effect measurement by ACCENT HL5500PC Hall system at room temperature, the sheet carriers concentration of 1kJ/m^2&250 shots irradiated sample is 5.08×10^{13} cm^{-2}, and the corresponding bulk carrier concentration are 1.69×10^{19} cm^{-3}. Therefore, the absorption coefficient for our experimental sample ($\sim 10^3$ cm^{-1}) remains more than one order of magnitude above these anticipated values ($\sim 10^2$ cm^{-1}). In other words, free carrier absorption itself cannot induce such large absorption coefficients. The absorption mechanism of S doped Si is the combination of multiple absorption contribution, these are sub-bandgap transition of S-related localized states, free carrier absorption, ion implantation induced defect absorption, and fs laser irradiation induced defect absorption.

An n^+-n junction photodiode based on S-doped Si after fs laser annealing layer (n$^+$-type, 1kJ/m^2&250 shots) layer and Si substrate (n-type) is prepared. The size of photodiode is 5 mm $\times$ 5 mm, aluminum (Al) film is evaporated onto front (comb) and back side (fully covered) to form Ohmic contact. Fig. 6(a) shows the diagram of Si photodiode. Fig. 6(b) shows the dark current and photocurrent
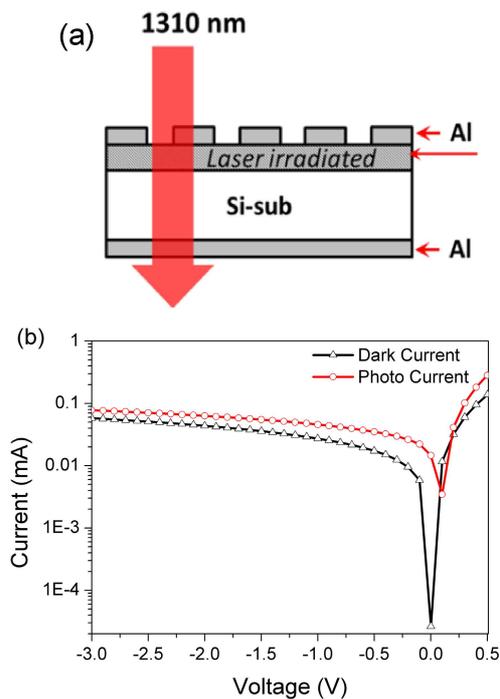
Fig. 6. (a) Illustration diagram of S-doped Si photodiode. (b) I-V curves (dark current and photo-current) of S-doped Si photodiode.

(1310 nm laser diode with 5 mW light power) of photodiode at room temperature. The dark current density of photodiode is calculated as 0.1 μA/cm^2. After illumination of 1310 nm wavelength, the photodiode can make a response with 4 mA/W@3 V and 8.4 mA/W@10 V reverse bias, respectively.

IV. Conclusions

In conclusion, supersaturated-doped Si samples with S are fabricated by ion implantation method. Fs laser irradiated annealing technique is used for improving the crystalline quality of implanted doping layer. Compared with the primary ion implanted Si sample, fs laser irradiated Si mainly has three excellent features. Initially, when annealing with proper laser fluence and deposited pulse number, the amorphous phase in ion implanted layer can be eliminated and recovered to crystalline Si. Furthermore, the absorptance below bandgap of Si irradiated by fs laser can be obviously increased and the absorption coefficient is 1.54×10^4 cm^{-1} at 1310 nm. The valid free carrier concentration in the supersaturated doping layer is lower than that of ns laser annealed samples. The photo-responses to 1310 nm light are 4 mA/W@3V and 8.4 mA/W@10V reverse bias of S-doped Si photodiode, respectively. As a result, the low free carrier concentration of the ion implanted Si irradiated by fs laser is beneficial to its application in infrared photo-detection.

References

[1] C. Wu *et al.*, "Near-unity below-band-gap absorption by microstructured silicon," *Appl. Phys. Lett.*, vol. 78, no. 13, pp. 1850–1852, Mar. 2001.

[2] H. Shao *et al.*, "Physical mechanisms for the unique optical properties of chalcogen-hyperdoped silicon," *Europhys. Lett.*, vol. 99, no. 4, p. 46005, 2012.

[3] X. Dong *et al.*, "A nitrogen-hyperdoped silicon material formed by femtosecond laser irradiation," *Appl. Phys. Lett.*, vol. 104, p. 091907, Mar. 2014.

[4] B. R. Tull, M. T. Winkler, and E. Mazur, "The role of diffusion in broadband infrared absorption in chalcogen-doped silicon," *Appl. Phys. A, Solids Surf.*, vol. 96, pp. 327–334, Aug. 2009.

[5] M. T. Winkler, D. Recht, M.-J. Sher, A. J. Said, E. Mazur, and M. J. Aziz, "Insulator-to-metal transition in sulfur-doped silicon," *Phys. Rev. Lett.*, vol. 106, p. 178701, Apr. 2011.

[6] T. G. Kim, J. M. Warrender, and M. J. Aziz, "Strong sub-band-gap infrared absorption in silicon supersaturated with sulfur," *Appl. Phys. Lett.*, vol. 88, no. 24, p. 241902, 2006.

[7] B. P. Bob *et al.*, "Fabrication and subband gap optical properties of silicon supersaturated with chalcogens by ion implantation and pulsed laser melting," *J. Appl. Phys.*, vol. 107, no. 12, p. 123506, 2010.

[8] I. Umezu *et al.*, "Emergence of very broad infrared absorption band by hyperdoping of silicon with chalcogens," *J. Appl. Phys.*, vol. 113, no. 21, p. 213501, 2013.

[9] H. S. Pan, D. Recht, S. Charnvanichborikarn, J. S. Williams, and M. J. Aziz, "Enhanced visible and near-infrared optical absorption in silicon supersaturated with chalcogens," *Appl. Phys. Lett.*, vol. 98, no. 12, p. 121913, 2011.

[10] Z. Huang, J. E. Carey, M. Liu, X. Guo, E. Mazur, and J. C. Campbell, "Microstructured silicon photodetector," *Appl. Phys. Lett.*, vol. 89, p. 033506, Jul. 2006.

[11] A. J. Said *et al.*, "Extended infrared photoresponse and gain in chalcogen-supersaturated silicon photodiodes," *Appl. Phys. Lett.*, vol. 99, no. 7, p. 073503, 2011.

[12] R. J. Younkin, "Surface studies and microstructure fabrication using femtosecond laser pulses," Ph.D. dissertation, Dept. Eng. Appl. Sci., Harvard Univ., Cambridge, MA, USA, 2001.

[13] Y. Gogotsi, C. Baek, and F. Kirscht, "Raman microspectroscopy study of processing-induced phase transformations and residual stress in silicon," *Semicond. Sci. Technol.*, vol. 14, no. 10, pp. 936–944, Jul. 1999.

[14] V. Domnich and Y. Gogotsi, "Phase transformations in silicon under contact loading," *Rev. Adv. Mater. Sci.*, vol. 3, no. 1, pp. 1–36, 2002.

[15] M. J. Smith, Y. T. Lin, M. J. Sher, M. T. Winkler, E. Mazur, and S. Gradečak, "Pressure-induced phase transformations during femtosecond-laser doping of silicon," *J. Appl. Phys.*, vol. 110, no. 5, p. 053524, 2011.

[16] Y. Mo, M. Z. Bazant, and E. Kaxiras, "Sulfur point defects in crystalline and amorphous silicon," *Phys. Rev. B, Condens. Matter*, vol. 70, p. 205210, Jun. 2004.

[17] J. F. Ziegler, M. D. Ziegler, and J. P. Biersack, "SRIM-the stopping and range of ions in matter (2010)," *Nucl. Instrum. Methods Phys. Res. B*, vol. 268, nos. 11–12, pp. 1818–1823, 2010.

[18] F. A. Trumbore, "Solid solubilities of impurity elements in germanium and silicon," *Bell Syst. Tech. J.*, vol. 39, no. 1, pp. 205–233, Jan. 1960.

[19] M. J. Sher, M. T. Winkler, and E. Mazur, "Pulsed-laser hyperdoping and surface texturing for photovoltaics," *MRS Bull.*, vol. 36, pp. 439–445, Sep. 2011.

[20] A. G. U. Perera, W. Z. Shen, W. C. Mallard, M. O. Tanner, and K. L. Wang, "Far-infrared free-hole absorption in epitaxial silicon films for homojunction detectors," *Appl. Phys. Lett.*, vol. 71, no. 4, pp. 515–517, 1997.

[21] W. Spitzer and H. Y. Fan, "Infrared absorption in *n*-type silicon," *Phys. Rev.*, vol. 108, no. 2, pp. 268–271, 1957.

Chun-Hao Li received the B.S. degree in microelectronics from the College of Electronic Science and Engineering, Jilin University, Changchun, China, in 2012. His current research interests modification and characterization of semiconductor surface.

Ji-Hong Zhao (M'17) received the B.S. degree in microelectronics and the Ph.D. degree from the College of Electronic Science and Engineering, Jilin University, Changchun, China, in 2006 and 2011, respectively. She is currently an Associate Professor with Jilin University. Her current research interests include analysis of properties of semiconductor surface by nonlinear optics, femtosecond laser micro- and nano-fabrication, and femtosecond laser-doping semiconductors.

Xin-Yue Yu received the B.S. degree in microelectronics from the College of Physics, Changchun University of Science and Technology, China, in 2015. She is currently pursuing the master's degree with the College of Electronic Science and Engineering, Jilin University, Changchun, China. She majors in microelectronics and solid-state electronics and her current research interest is semiconductor's doping by femtosecond laser irradiation.

Qi-Dai Chen received the B.S. degree in physics from the University of Science and Technology of China, Hefei, China, in 1998, and the Ph.D. degree from the Institute of Physics, Chinese Academy of Sciences, Beijing, China, in 2004. He was a Post-Doctoral Research Associate at Osaka City University, Osaka, Japan, from 2005 to 2006. He is currently a Professor with Jilin University, Changchun, China. His current research interests include laser microfabrication, ultrafast laser spectroscopy, photochemistry, and photophysics.

Jing Feng received the B.S. and Ph.D. degrees in microelectronics and solid-state electronics from Jilin University, Changchun, China, in 1997 and 2003, respectively. From 2003 to 2006, she was a Post-Doctoral Researcher at RIKEN, Japan. In 2006, she joined Jilin University, where she is currently a Professor with the College of Electronic Science and Engineering and the State Key Laboratory on Integrated Optoelectronics. She has published more than 100 scientific papers in academic journals. Her research interest includes organic optoelectronic devices.

Pei-De Han received the B.S. degree in radio physics from Nankai University, Tianjin, China, in 1981, and the Ph.D. degree from the Vienna University of Technology, Vienna, Austria, in 1996. From 1996 to 1997, he was a Post-Doctoral Researcher at the Institute of Semiconductors, Chinese Academy of Sciences, China. In 1997, she joined the Institute of Semiconductors, Chinese Academy of Sciences, where he is currently a Professor with the State Key Laboratory on Integrated Optoelectronics. He has published more than 80 scientific papers in academic journals. His research interest includes photovoltaic devices.

Hong-Bo Sun received the B.S. and Ph.D. degrees in optoelectronics from Jilin University, China, in 1992 and 1996, respectively. He was a Post-Doctoral Researcher with the University of Tokushima, Japan, from 1996 to 2000, and then as an Assistant Professor at the Department of Applied Physics, Osaka University, Osaka, Japan. In 2005, he was promoted to a Full Professor (Changjiang Scholar Professor) with Jilin University. His research interests have been laser nanofabrication and ultrafast spectroscopy: fabrication of various microoptical, microelectronical, micromechanical, microoptoelectronic, microfluidic components and integrated systems at nanoscales, and exploring ultrafast dynamics of photons, electrons, phonons, and surface plasmons in solar cells, organic light-emitting devices, and low-dimensional quantum systems at femtosecond timescale. He has authored more than 300 scientific papers and delivered more than 150 invited talks at international conferences. The total SCI citations to his papers are around 10 000 times. He also served as the General/Technical Co-Chairs of a large number of conferences.